Structural and Fluorescence Studies of Polycrystalline α-Al$_2$O$_3$ Obtained From Sulfuric Acid Anodic Alumina

Katsiaryna Chernyakova,* Renata Karpicz, Danielis Rutkauskas, Igor Vrublevsky, and Achim Walter Hassel

In the present study, robust α-Al$_2$O$_3$ specimens (144 μm thick) are obtained by the heat treatment at 1400 °C of free-standing sulfuric acid anodic alumina. Scanning electron microscopy analysis show that the as-anodized anodic alumina films possess well-ordered porous structure with the pore diameter of about 10.2 nm. After heat treatment at 1400 °C the samples lose their porous structure and certain crystallites with average size of 5–6 μm can be observed. These crystallites can be visualized by fluorescence imaging. According to differential scanning calorimetry data accomplished by X-ray analysis, the first step of crystallization occurs at around 967 °C, producing γ-Al$_2$O$_3$. The second one takes place at around 1194 °C, which corresponds to the formation of α-Al$_2$O$_3$. For the as-anodized and samples treated at temperatures below 1200 °C the band at 420 nm can be attributed to the emission of OH-related and other impurities centers. The fluorescence at 460 nm relates to emission of oxygen defect centers, such as F and F$_2$ centers, and sharp bands at 678 and 693 nm indicate the formation of highly crystalline alumina. For α-Al$_2$O$_3$, its fluorescence is caused by both surface defects and oxygen defect centers. The fluorescence spectroscopy can be applied as a cheap, fast, nondestructive method for the identification of amorphous alumina crystallization.

1. Introduction

Porous oxide materials have attracted considerable attention due to their potential applications in filters, catalyst support, electronic, magnetic and optical devices. It is also known, α-Al$_2$O$_3$ membranes due to their biocompatibility and high chemical resistance are of great demand.[1] One of the widely applied methods for alumina formation is aluminum anodizing in aqueous acidic solutions.[2] However, as-anodized anodic

Dr. K. Chernyakova, Dr. I. Vrublevsky
Belarusian State University of Informatics and Radioelectronics
P. Brovka, 6, Minsk, Belarus
E-mail: katsiarynacher@bsuir.by

Dr. R. Karpicz, Dr. D. Rutkauskas
Center for Physical Science and Technology
Sauletekio av. 3, Vilnius, Lithuania

Prof. A. W. Hassel
Johannes Kepler University Linz
Institute of Chemical Technology of Inorganic Materials
Altenbergerstrasse 69, Linz, Austria

alumina is amorphous, and in fact, it is fragile and susceptible to both acid and base attack. The product of electrochemical oxidation of aluminum has a variable composition (Al$_2$O$_3 \cdot n$H$_2$O or AlOOH). That is, anodic alumina contains water, hydroxyl groups, and electrolyte ions.[3,4] Therefore, to improve its properties and extend the field of its application the high temperature treatment is required.

During high temperature treatment the desorption and decomposition of the impurities as well as changes in alumina density cause curving and cracking of the samples. In previous studies it was shown that flat α-Al$_2$O$_3$ films could be synthesized from phosphoric and oxalic acid anodic alumina where the anion-containing layer was deleted in order to prevent thermal deformation, but the size of the samples was quite small, less than 1 cm^2.[5] In Ref. [1] authors obtained porous α-Al$_2$O$_3$ membranes of 25 mm diameter without thermal deformation, initial samples were synthesized in oxalic and phosphoric acids. At the same time, sulfuric acid is one of the cheapest electrolytes among the others commercially applied.[6] However, due to high porosity and anion content (10–13%) in as-anodized sulfuric acid anodic alumina the formation of flat and large α-Al$_2$O$_3$ films from free-standing anodic alumina samples remains quite a challenge.[7]

Porous alumina films also show fluorescence properties, which justify their employment as templates for synthesis of variety of new optical materials.[8,9] The fluorescence properties of porous anodic aluminum oxide films are determined not only by their structural features, the nature of the defects, but also by the presence of impurities, such as anions of the electrolyte.[10] The origin of the emission centers in both the as-anodized and heat treated anodic alumina is widely discussed.[11–13] G.S Huang et al. found that fluorescence at about 465 nm of porous anodic alumina formed in sulfuric acid is caused by the oxygen vacancies in the membrane and another blue emission band in the 400–440 nm region is attributed to the optical transition in the isolated OH groups at the surface.[14] Other scientists found that fluorescence band in the 400–440 nm is typical for embedded impurities such as malonate and tartarate ions.[15–18] Various metal oxides also showed the same photoluminescence of OH-related centers in

oxidized nanocrystalline and porous silicon, hydrated alumina oxide, hydrated lead oxide and zinc oxide.[19] In as-anodized anodic alumina and in α-Al_2O_3, fluorescence at about 400–440 and 500 nm can be also attributed to F and F_2 centers, respectively.[12,17,20–23]

In the present study, we obtained robust α-Al_2O_3 samples with size of 2.6 cm^2 and thickness of 144 μm by the heat treatment at 1400 °C of free-standing sulfuric anodic alumina specimens and investigated their physical, chemical and fluorescence properties.

2. Experimental Section

2.1. Anodizing

The high-purity aluminum foil (99.99 wt.%, 100 μm thick, 13 × 20 mm, AlfaAesar) was used as a starting material. The aluminum specimens were pretreated in a hot solution of 1.5 M NaOH for 15 s, neutralized in 1.5 M HNO_3 for 2 min, then carefully rinsed in distilled water and air-dried. Anodic alumina was formed by double-sided anodizing of aluminum specimens in the 2.0 M aqueous solution of sulfuric acid at the constant current density of 320 $A\,m^{-2}$ up to the moment when the aluminum was completely oxidized. At the steady state of oxide growth the voltage was about 20 V. The anodizing process was carried out in two-electrode glass cell, in which platinum grid was used as a counter electrode. The solution was stirred by a magnetic stirrer, and the temperature was maintained at a constant value of (10.0 ± 0.1) °C by cryostat FT 901 (Julabo). The anodizing process was controlled by a direct current power supply NTN 700–125 (FuG Elektronik). If indicated, the samples were annealed in temperature range of 800–1400 °C in air in programmable muffle HTCT 03/16 (Nabertherm). The temperature was gradually increased from room temperature up to 800 °C and then from 800 to 1400 °C at a heating rate of about 100 °C h^{-1} to prevent thermal cracking and curling.

2.2. Characterization

Surface morphology and cross-section both of the as-anodized and of the heat treated anodic alumina specimens were analyzed by scanning electron microscopy (SEM) on a LEO 1550 VP (Leo Electron microscope). Image analysis was performed by ImageJ software.

To evaluate the structures of amorphous samples thermogravimetry − differential scanning calorimetry (TG-DSC) technique was applied using STA 449C Jupiter (Netzsch) equipment. A total of 30 g of the powdered sample was placed in alumina pan and then heated from 30 to 1250 °C at heating rate of 10 °C min^{-1} under protection of argon (60 mL min^{-1}).

The crystal structure of the heat treated samples was studied by X-ray diffraction (XRD) patterns. The equipment used was X-Pert Pro diffractometer (Phillips) with CuK_α radiation ($\lambda = 1.5406$ Å) in 2θ range of 20–100°. Crystalline phases were identified and indexed by means of X-ray Diffraction Philips Analytical software and the PCPDFWIN database − JCPDS-ICDD.

2.3. Fluorescence Properties

Fluorescence imaging was carried out with fluorescence microscope Eclipse Ti (Nikon) with two-channel (430–480 nm)/ (485–630 nm) spectral detection at $\lambda_{ex} = 405$ nm. Fluorescence spectra and kinetics were measured with a time-correlated single photon counting spectrometer Edinburg-F900 (Edinburg instruments). A picosecond pulsed diode laser EPL-375 emitting picosecond (76 ps) duration pulses was used for the excitation at 375 nm with an average power of 0.10 mW mm^{-2}. The pulse repetition rate was 1 MHz and the time resolution of the setup was about 100 ps taking into account temporal deconvolution procedure. All fluorescence spectra were corrected for the instrument sensitivity. We applied the ultrapure alpha-alumina powder (99.99%, average particle size 1–2 mm, Inframat, advanced materials) as reference material to compare the fluorescence properties of the samples obtained with commercially synthesized ones.

3. Results and Discussion

3.1. Surface Characterization and Mechanical Properties

The as-anodized sulfuric acid anodic alumina samples are transparent (154 μm thick) with light-grey color due to residual aluminum. After the heat treatment at 1100 °C it turned translucent. At 1400 °C film became white and non-transparent, its thickness decreases to 144 μm, as during crystallization alumina compaction takes place. However, under the chosen heat treatment conditions neither cracking nor curling are observed and the samples retain their original planarity (**Figure 1**).

According to the SEM studies, the as-anodized anodic alumina films possess ordered porous structure with the pore diameter 10.2 nm (**Figure 2**a). A total of 1400 °C-treated samples almost lose their initial porous structure due to crystallization and compaction of amorphous alumina. On the surface of 1400 °C-treated anodic alumina penta- and hexagon-shaped crystallites of uniform average 5–6 μm size can be observed. Grain boundaries are transition layers with thickness 0.3–0.4 μm (Figure 2b). Both on the surface and in the bulk of anodic alumina there are just certain microvoids irregularly shaped with
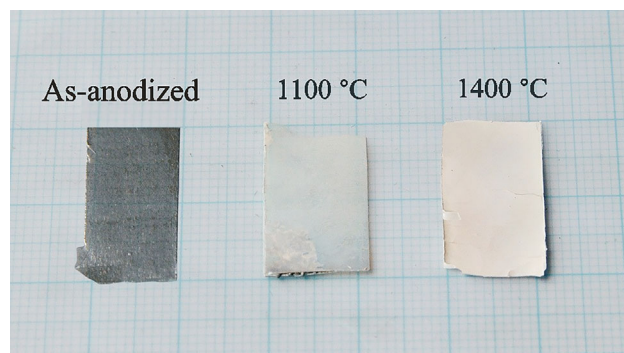
Figure 1. Surface appearance of the as-anodized and heat treated at 1100 and 1400 °C alumina films formed in sulfuric acid.
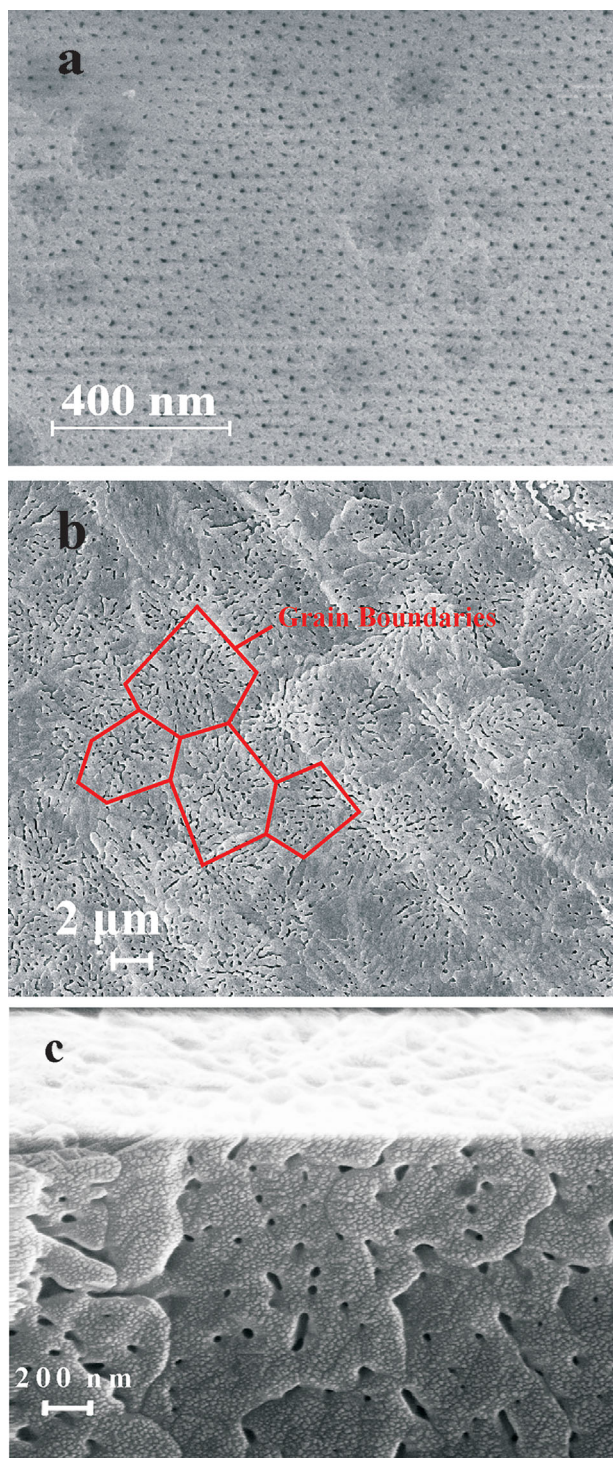
Figure 2. SEM images of the surface (a) of as-anodized sulfuric acid anodic alumina; surface (b) and cross-section (c) of the heat treated at 1400 °C in air anodic alumina formed in sulfuric acid.

the size of more than 100 nm formed between the different grains. As can be seen from Figure 2c, the alumina compaction occurred uniformly throughout the sample. According to Ref. [24], the shape of the obtained crystallites indicates the formation of equilibrium-shaped crystals of α-Al$_2$O$_3$. The

appearance of the crystallites of the 1400 °C-treated samples can be easily asserted by fluorescence microscopy, λ$_{ex}$ = 405 nm (**Figure 3**a). The as-anodized anodic alumina has uniform emission throughout the surface. At the same time, the 1400 °C-treated sample mainly emits only along the grain boundaries (Figure 3b), as during crystallization defects in α-Al$_2$O$_3$ concentrate namely on the surface. For example, hydroxyl groups bound to a surface aluminum ion which also contribute to the luminescence process.[25] In porous anodic alumina the surface structure transformation during high temperature treatment is caused by the reorganization of oxygen and aluminum sub-lattice and removal of impurities incorporated during anodizing.

3.2. Phase Characterization

A mass loss of 3.3% in temperature range of 30–950 °C indicates dehydration and dehydroxilation processes, that is, deletion of physically and chemically adsorbed water and hydroxyl species.[26] The mass loss of 9.5% at around 967–972 °C corresponds to the release of SO$_2$ and O$_2$. [27–32] And then the gradual mass loss, corresponding to the SO$_2$ release,[29] of about 4.3% total is observed in the temperature range of 980–1250 °C (**Figure 4**).

DSC curve shows a very sharp exothermic peak at around 967 °C and another broader peak onset at around 1194 °C (see Figure 4). The first exothermic peak indicates the beginning of the γ-Al$_2$O$_3$ crystallization. The second exothermic peak associated with the formation of α-Al$_2$O$_3$. The exotherm at 967 °C is followed by an endotherm. This endothermic peak, which is more pronounced at low heating rates, was previously observed in DSC curves of sulfuric acid anodic alumina and can be attributed to the decomposition of SO$_4^{2-}$ ions and their consecutive release as SO$_2$ and O$_2$.[31] Our results agree with previous thermal analysis data obtained by Ozao et al.[27] and Brown et al.[31] As anodic alumina formed in sulfuric acid contains 8–17 mass.% of sulfur[4] it stabilizes the amorphous alumina matrix and, as a result, the onset temperature for γ-Al$_2$O$_3$ formation is higher than that for amorphous alumina obtained by chemical methods.[33,34]

To study the crystallization of sulfuric acid anodic alumina the XRD analysis was carried out. The as-anodized and 800 °C-treated anodic alumina specimens are essentially X-ray amorphous (**Figure 5**). With a treatment at 900–1000 °C the only γ-Al$_2$O$_3$ phase (JCPDS 10–0425) with well defined peaks at 2θ = 37.5, 45.9, and 67.1 is observed. The unit cell dimensions are: $a = b = c = 7.89$ Å (**Table 1**). At 1100 °C the phases of γ-, θ-, and α-Al$_2$O$_3$ co-exist, but α-Al$_2$O$_3$ (JCPDS 46–1212) prevails. The small amount of θ-Al$_2$O$_3$ phase (JCPDS 35–0121) can be identified by the following peaks at 2θ = 32.8 and 35.2 presented in XRD pattern. The unit cell dimensions for 1100 °C-treated α-Al$_2$O$_3$ are: $a = b = 4.76$ Å, $c = 13.00$ Å. After heat treatment at 1200–1400 °C only well defined peaks of α-Al$_2$O$_3$ phase are identified ($a = b = 4.76$ Å, $c = 12.99$ Å). The cell parameters for 1400 °C-treated alumina completely coincide with reference data. It should be also emphasized that high resolution of $K_{\alpha 1}$ and $K_{\alpha 2}$ lines in the large 2θ region indicates that the equilibrium phase of α-Al$_2$O$_3$ was
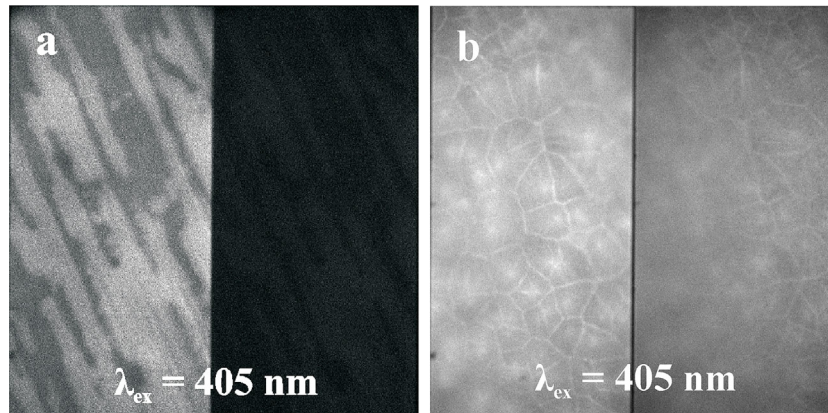
Figure 3. Appearance (200 × 100 μm) in the fluorescence microscope of the as-anodized (a) and (b) of the heat treated at 1400 °C in air anodic alumina film formed in sulfuric acid in (430–480 nm)/(485–630 nm) range under 405 nm excitation.

obtained and it agrees with the formation of equilibrium-shaped crystals.[27–34]

3.3. Fluorescence Properties

According to the steady-state fluorescence measurements ($\lambda_{ex} = 375$ nm) the as-anodized and heat treated films are characterized by a broad fluorescence in the wavelength range of 400–650 nm and sharp peaks around 678 and 694 nm in the anodic alumina treated at temperatures above 1000 °C. All spectra were normalized to their maximum intensity, for better qualitative comparison. Broad fluorescence have at least two components: one fluorescence band with peak at about 420 nm and another at about 460 nm. With increased treatment temperature to 1000 °C the position of emission maximum slightly redshifts from 444 to 462 nm. The spectrum

of 1400 °C-treated sample is almost identical to the one of ultrapure α-Al₂O₃ (**Figure 6**a).

For samples treated at temperatures above 1000 °C one can see two sharp intensive peaks at around 678 and 693 nm. Most investigations report that there are Cr^{3+} or Mn^{4+} ions in crystalline alumina and associate these bands with the emission of the ions.[22,35,36] In our case it is doubtful, as we used highly pure aluminum foil and double distilled water in the experiments. Moreover, in the fluorescence spectrum of purchased ultrapure α-Al₂O₃ these bands are also presented. Therefore, according to our and a very few previous data[35] these bands can be associated with single-crystalline sapphire crystal having highly crystalline order. This also confirms XRD data that indicate the formation of equilibrium phase of α-Al₂O₃ at 1400 °C.

The time-resolved fluorescence data show that with increased treatment temperature the average life time of the fluorescence
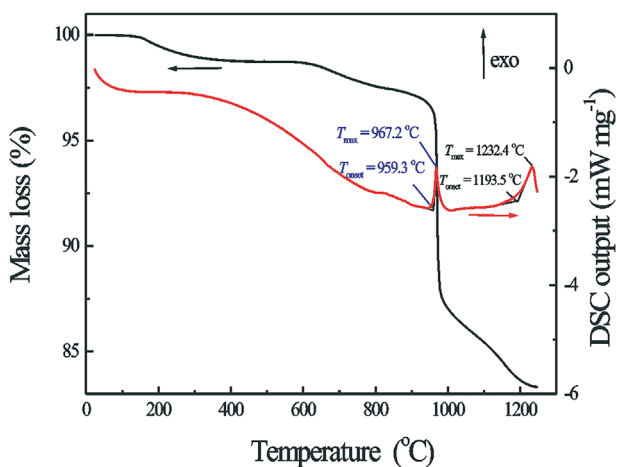
Figure 4. TG-DSC plot for sulfuric acid anodic alumina.
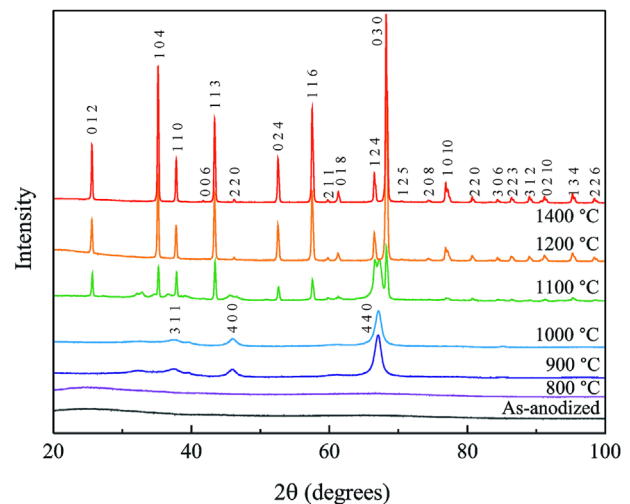
Figure 5. XRD for the as-anodized and heat treated at 800–1400 °C in air anodic alumina films formed in sulfuric acid.

Table 1. XRD data for the as-anodized and heat treated at 800–1400 °C in air anodic alumina films formed in sulfuric acid.

Sample	Phase	JCPDS	Lattice constant, Å	Space group
As-anodized	Amorphous	–	–	–
800 °C-treated	Amorphous	–	–	–
900 °C-treated	γ-Al$_2$O$_3$	10-0425	$a = 7.89$	Fd3m
1000 °C-treated	γ-Al$_2$O$_3$	10-0425	$a = 7.89$	Fd3m
1100 °C-treated	α-Al$_2$O$_3$ (γ-and θ-Al$_2$O$_3$)	46-1212	$a = 4.76$; $c = 13.00$	R3c
1200 °C-treated	α-Al$_2$O$_3$	46-1212	$a = 4.76$; $c = 13.01$	R3c
1400 °C-treated	α-Al$_2$O$_3$	46-1212	$a = 4.76$; $c = 12.99$	R3c

rises from 3.5 to 4.9 ns (Figure 6b, **Table 2**). For the as-anodized the first life time (τ_1) is about 0.6 ns and it does not change with increased treatment temperature from 800 to 1000 °C. At the same time, its relative contribution to the total fluorescence has a tendency to decrease from 24 (as-anodized alumina) to 19% (1000 °C). For 1400 °C-treated alumina and ultrapure α-Al$_2$O$_3$

$\tau_1 = 0.8$ ns. As concerning τ_2 and τ_3 they also have tendency to increases with increased treatment temperature. Their values vary in the range 2.2–3.7 and 6.9–8.2 ns, respectively. The correlation in changes in relative contribution is not observed. However, one can see, that for 900 °C-treated sample all three life times are the short among the other samples and for τ_1 and τ_2 the relative contributions are also the shortest. For example, the contribution of τ_1 and τ_2 is by 6 and 10% lower than for the as-anodized sample, respectively. Nevertheless, the relative contribution of τ_3 is by 16% higher than for the as-anodized sample. These observations agree with DTA and XRD data and are the evidences of the amorphous alumina crystallization into γ-Al$_2$O$_3$. At 1400 °C, τ_2 increases in 1.0 ns and τ_3 in 0.7 ns comparing with 1100 °C-treated alumina. However, in this case both life times and relative contributions are not very different from ultrapure α-Al$_2$O$_3$.

Ruckschloss et al.[19] established that life time for OH-related fluorescence is about several nanoseconds. At the same time, the F centers fluorescence decay is usually nonexponential and shorter than 7 ns.[37] Consequently, we can conclude that for as-anodized and samples treated at temperatures below 1200 °C the band at 420 nm can be attributed to the emission of OH-related centers and other impurities.[38,39] The fluorescence at 460 nm relates to emission of oxygen defect centers, such as F and F_2 centers, and bands at 678 and 693 nm are characteristic for the formation of highly crystalline alumina. For α-Al$_2$O$_3$ the situation is relatively different, as in the case of α-Al$_2$O$_3$ the
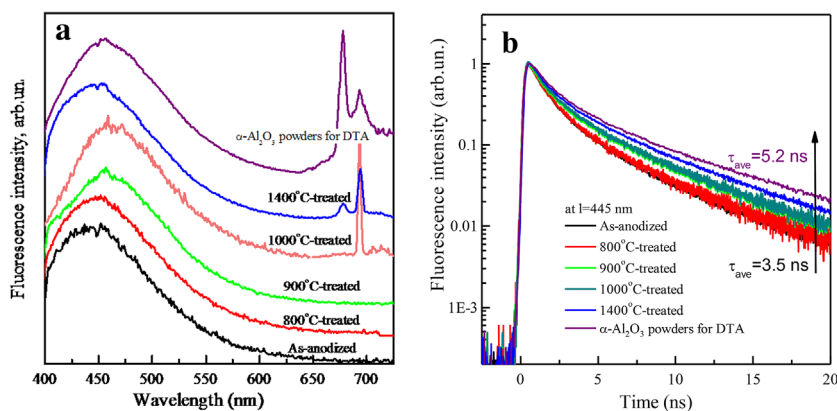
Figure 6. Steady-state (a) and time-resolved kinetics registered in the maximum intensity (b) fluorescence spectra of the as-anodized and heat treated at various temperatures in air anodic alumina film formed in sulfuric acid, $\lambda_{ex} = 375$ nm.

Table 2. Fluorescence data for the as-anodized and heat treated at 800–1400 °C in air anodic alumina films formed in sulfuric acid.

Sample	λ_{em}, nm	τ_1, ns (%)	τ_2, ns (%)	τ_3, ns (%)	τ_{ave}, ns (%)
As-anodized	444	0.6 (24%)	2.3 (45%)	7.4 (31%)	3.5
800 °C-treated	450	0.6 (20%)	2.6 (43%)	7.3 (37%)	3.9
900 °C-treated	458	0.5 (18%)	2.2 (35%)	6.9 (47%)	4.1
1000 °C-treated	462, 693	0.6 (19%)	2.7 (40%)	7.3 (41%)	4.2
1400 °C-treated	447, 678, 694	0.8 (22%)	3.7 (38%)	8.2 (40%)	4.9
α-Al$_2$O$_3$ powders	455, 678, 694	0.8 (20%)	3.6 (41%)	9.2 (39%)	5.2

ADVANCED
SCIENCE NEWS
www.advancedsciencenews.com

physica
pss
status
solidi a
www.pss-a.com

presence of OH groups and water is not possible and during crystallization the crystalline structure changes drastically, so, we believe its fluorescence is caused by both surface defects (See Figure 3b) and oxygen defect centers. Moreover, fluorescence spectroscopy as a cheap, fast, nondestructive method can be used for the identification of amorphous alumina crystallization.

4. Conclusions

It was shown that the as-anodized sulfuric acid anodic alumina possesses ordered porous structure with the pore diameter of about 10.2 nm. After heat treatment at 1400 °C the samples lose their porous structure and certain crystallites with average size of 5–6 μm can be observed. These crystallites can be visualized by fluorescence imaging. By TG–DSC technique accomplished by X-ray analysis it was established that the first step of crystallization occurs at around 967 °C, producing γ-Al$_2$O$_3$. The second one takes place at around 1194 °C, which corresponds to the formation of α-Al$_2$O$_3$. For the as-anodized and samples treated at temperatures below 1200 °C the band at 420 nm can be attributed to the emission of OH-related centers and other impurities. The fluorescence at 460 nm relates to emission of oxygen defect centers, such as F and F$_2$ centers. For α-Al$_2$O$_3$, its fluorescence is caused by both surface defects and oxygen defect centers that are mainly located at grain boundaries. It was also shown that using characteristic emission bands at 678 and 693 nm the fluorescence spectroscopy can be applied as a cheap, fast, nondestructive method for the identification of amorphous alumina crystallization.

Conflict of Interest

The authors declare no conflict of interest.

[1] T. Masuda, H. Asoh, S. Haraguchi, S. Ono, *Materials* **2015**, *8*, 1350.
[2] W. Lee, S. J. Park, *Chem. Rev.* **2014**, *114*, 7487.
[3] Y. Yamamoto, N. Baba, *Thin Solid Films* **1983**, *101*, 329.
[4] G. E. Thompson, G. C. Wood, *Treatise on Materials Science and Technology*, Vol. *23*, J.C. Scully, (Ed.), Academic Press, New York **1983**, p. 205.
[5] Y. Chang, Z. Ling, Y. Liu, X. Hu, Y. Li, *J. Mater. Chem*. **2012**, *22*, 7445.
[6] T. Kikuchi, D. Nakajima, O. Nishinaga, S. Natsui, R. O. Suzuki, *Curr. Nanosci*. **2015**, *11*, 560.
[7] G. D. Sulka, *Nanostructured Materials in Electrochemistry*, A. Eftekhari (Ed.), Wiley-VCH Verlag GmbH & Co. KGaA, Weinheim, Germany **2008**, pp. 111.
[8] A. V. Kukhta, G. G. Gorokh, E. E. Kolesnik, A. I. Mitkovets, M. I. Taoubi, Y. A. Koshin, A. M. Mozalev, *Surf. Sci*. **2002**, *507–510*, 593.
[9] S. K. Lazarouk, A. V. Mudryi, A. V. Ivanyukovich, A. A. Leshok, D. N. Unuchek, V. A. Labunov, *Semiconductors* **2005**, *39*, 891.
[10] S. Stojadinovich, R. Vasilic, *Curr. Nanosci*. **2015**, *11*, 547.
[11] W. L. Xu, M. J. Zheng, S. Wu, S. Shen, *Appl. Phys. Lett*. **2004**, *85*, 4364.
[12] Zh. Li, K. Huang, *J. Lumin*. **2007**, *127*, 435.
[13] M. D. Yang, K. W. Chen, J. L. Shen, J. C. Wang, C. Hsu, *Nanotechnology* **2007**, *18*, 405707.
[14] G. S. Huang, X. L. Wu, G. G. Siu, P. K. Chu, *Solid State Commun*. **2006**, *137*, 621.
[15] C. Lin, M. Yu, Z. Cheng, C. Zhang, Q. Meng, J. Lin, *Inorg. Chem*. **2008**, *47*, 49.
[16] I. Vrublevsky, A. Jagminas, S. Hemeltjen, W. A. Goedel, *Appl. Surf. Sci*. **2010**, *256*, 2013.
[17] A. Brzozka, A. Brudzisz, K. Hnida, G. D. Sulka, Chemical and structural modifications of nanoporous alumina and its optical properties. (Eds: Losic D., Santos A.) *Electrochemically Engineered Nanoporous Materials*. Springer Series in Materials Science, Springer, Cham, Vol. *220*, **2015**.
[18] K. Chernyakova, R. Karpicz, S. Zavadski, O. Poklonskaya, A. Jagminas, I. Vrublevsky, *J. Lumin*. **2017**, *182*, 233.
[19] M. Rückschloss, Th. Wirschem, H. Tamura, G. Ruhl, J. Oswald, S. Veprek, *J. Lumin*. **1995**, *63*, 279.
[20] V. S. Kortov, A. E. Ermakov, A. F. Zatsepin, S. V. Nikiforov, *Radiat. Meas*. **2008**, *43*, 341.
[21] B. D. Evans, *J. Nuclear Mater*. **1995**, *219*, 202.
[22] D. Abdelkader, B. Abdecharif, Peculiarity of the cathodoluminescence of alpha-alumina prepared by calcination of gibbsite powder or generated by oxidation of a metallic fecral alloy, *cathodoluminescence*, (Eds: N. Yamamoto), InTech, Rijeka **2012**, p. 324.
[23] M. Itou, A. Fujiwara, T. Uchino, *J. Phys. Chem. C* **2009**, *113*, 20949.
[24] E. R. Dobrovinskaya, L. A. Lytvynov, V. Pishchik, *Sapphire: Material, Manufacturing, Applications*, Springer Science Business Media, NY **2009**, p. 481.
[25] A. Amirsalari, S. F. Shayesteh, *Superlattice. Microstr*. **2015**, *82*, 507.
[26] I. Vrublevsky, K. Chernyakova, A. Bund, A. Ispas, U. Schmidt, *Appl. Surf. Sci*. **2012**, *258*, 5394.
[27] R. Ozao, M. Ochiai, N. Ichimura, H. Takahashi, T. Inada, *Thermochim. Acta* **2000**, *352–353*, 91.
[28] R. Ozao, M. Ochiai, H. Yoshida, Y. Ichimura, T. Inada, *J. Therm. Anal. Cal*. **2001**, *64*, 923.
[29] R. Ozao, H. Yoshida, T. Inada, *J. Thermal Anal. Calorim*. **2002**, *69*, 925.
[30] M. E. Mata-Zamora, J. M. Saniger, *Rev. Mex. Fıs*. **2005**, *51*, 502.
[31] I. W. N. Brown, J. P. Wu, G. Smith, Fabrication, structure and properties of nanostructured ceramic membranes, *ceramic materials—progress in modern ceramics*, (Ed. F. Shi), InTech, Rijeka **2012**, p. 191.
[32] I. W. M. Brown, M. E. Bowden, T. Kemmitt, K. J. D. MacKenzie, *Curr. Appl. Phys*. **2006**, *6*, 557.
[33] T. M. H. Costa, M. R. Gallas, E. V. Benvenutti, J. A. H. da Jornada, *J. Phys. Chem. B* **1999**, *103*, 4278.
[34] M. R. Gallas, B. Hockey, A. Pechenik, G. J. Piermarini, *J. Am. Ceram. Soc*. **1994**, *77*, 2107.
[35] P. G. Li, M. Lei, W. H. Tag, *Mater. Lett*. **2010**, *64*, 161.
[36] R. Krishnan, R. Kesavamoorthy, S. Dash, A. K. Tyagi, B. Raj, *Scr. Mater*. **2003**, *48*, 1099.
[37] W. J. Stępniowski, M. Norek, M. Michalska-Domańska, A. Nowak-Stępniowska, M. Kaliszewski, P. Chilimoniuk, A. Bombalska, Z. Bojar, *J. Mater. Sci. Nanotech*. **2014**, *1*.
[38] M. Breysse, G. Coudurier, B. Claudel, L. Faure, *J. Lumin*. **1982**, *26*, 239.
[39] L. El Mir, A. Amlouk, C. Barthou, *J. Phys. Chem. Solids* **2006**, *67*, 2395.